Comparison of the spherically averaged pseudopotential model with the stabilized jellium model

Armando Vieira†, M Begoña Torres‡, Carlos Fiolhais† and L Carlos Balbás‡

† Departamento de Fisica da Universidade de Coimbra, P-3000 Coimbra, Portugal
‡ Departamento de Física Teórica, Universidad de Valladolid, E-47011 Valladolid, Spain

Abstract. We compare Kohn–Sham results (density, cohesive energy, size and effect of charging) of the spherically averaged pseudopotential model with the stabilized jellium model for clusters of sodium and aluminium with less than 20 atoms. We find that the stabilized jellium model, although conceptually and practically simpler, gives better results for the cohesive energy and the elastic stiffness. We use the local density approximation as well as the generalized gradient approximation for the exchange and correlation energies.

1. Introduction

The energy functional for an electronic system under the influence of a positive charge distribution (ions) is

$$E[n, n_+] = T[n] + E_{xc}[n] + \frac{1}{2} \int d^3r \int d^3r' \frac{n(r)n(r')}{|r - r'|}$$
$$+ \int d^3r \, V_+(r)n(r) + \frac{1}{2} \int d^3r \int d^3r \frac{n_+(r)n_+(r')}{|r - r'|} \quad (1)$$

where $n(r)$ is the density of the valence electrons, $n_+(r)$ is the ionic density, T is the kinetic energy, E_{xc} is the exchange and correlation energy and $V_+(r)$ is the potential created by the ions. Atomic units are used throughout this paper.

The jellium model is a simple model to describe simple metals. To study a spherical cluster in this model, the ions are replaced by a continuous positive background which is constant inside a sphere of radius $R_{jel} = r_s N^{1/3}$, where N is the number of valence electrons, and zero outside:

$$n_+(r) = \bar{n}\theta(R_{jel} - r) \quad (2)$$

with $\bar{n} = 3/(4\pi r_s^3)$. For this model the external potential is simply

$$V_+(r) \equiv v_{jel}(r) = \begin{cases} -\dfrac{N}{2R_{jel}}\left[3 - \left(\dfrac{r}{R_{jel}}\right)^2\right] & (r < R_{jel}) \\ -\dfrac{N}{r} & (r \geqslant R_{jel}). \end{cases} \quad (3)$$

The stabilized jellium model (SJM) [1] represents an improvement over the jellium model. For bulk matter, it yields more realistic binding energies and bulk moduli [1]. For semi-infinite systems, it provides more correct surface energies and work functions [2].

For clusters, it gives very reasonable cohesive energies, dissociation energies, ionization energies, etc [3, 4]. Its energy functional may be written as

$$E_{SJ}[n, n_+] = E_J[n, n_+] + \langle \delta v \rangle \int d^3 r \, \theta(r - R_{jel})[n(r) - n_+(r)] + \tilde{\epsilon} \int d^3 r \, n_+(r) \qquad (4)$$

where $E_J[n, n_+]$ is the jellium energy functional (equation (1) with the external potential given by equation (3)) and

$$\langle \delta v \rangle = \frac{1}{v} \int_0^{r_0} dr \, r^2 [w(r) - v_{jel}(r)] = -\frac{3}{10} \frac{v^{2/3}}{r_s} + \frac{3}{2} \frac{r_c^2}{r_s^3} \qquad (5)$$

is the average, in the Wigner–Seitz cell (taken to be a sphere of radius $r_0 = r_s v^{1/3}$, with v the valence), of the difference between the pseudopotential

$$w(r) = \begin{cases} 0 & (r < r_c) \\ -v/r & (r \geqslant r_c) \end{cases} \qquad (6)$$

(Ashcroft empty core potential [5], with core radius r_c) and the jellium potential. In the last term of equation (4), $\tilde{\epsilon}$ is the spurious background repulsion inside each Wigner–Seitz cell, which is equal to the sum of the Madelung energy

$$\epsilon_M = \frac{1}{v} \int_0^{r_0} dr \, 4\pi r^2 \bar{n} \left(\frac{-v}{r} + \frac{1}{2} v_{jel} \right) = -\frac{9}{10} \frac{v^{2/3}}{r_s} \qquad (7)$$

and the average of the pseudopotential repulsion [1]:

$$\frac{1}{v} \int_0^{r_c} dr \, 4\pi r^2 \bar{n} \frac{v}{r} = \frac{3}{2} \frac{r_c^2}{r_s^3}. \qquad (8)$$

Physically, equation (4) means that we start with the jellium model and localize the ions uniformly, but their interaction with the valence electrons (accounted for by the pseudopotential) is only taken into account perturbatively and in a spherically averaged way.

With the energy functional (4) we may extract results for clusters, via the Kohn–Sham method in the local density approximation (LDA) for exchange and correlation, going from the single stabilized jellium atom all the way up to the bulk solid. We use the Perdew–Wang interpolative formula [6] for the correlation energy. We consider that the jellium background is either fixed with the bulk density value or relaxed in order to give the minimal energy for a given number of particles (using a fixed pseudopotential, e.g. transferred from the bulk). In the latter case, which is in principle more realistic, we speak of self-compression of the neutral cluster, a phenomenon which may be explained classically by the effect of the surface tension on the density [7–9]. Here we take, when not otherwise indicated, the SJM including self-compression. The energetics of the cluster ground states is similar to that of the jellium model, with the same shell structure, but shifted down, i.e. the valence electrons are more bound.

Let $E = E(N, r_s, r_c, v)$ be the binding energy of a neutral spherical cluster with N valence electrons. The equilibrium ionic density, r_s^*, of a cluster is obtained by imposing the following equilibrium condition:

$$\frac{\partial}{\partial r_s} \left[\frac{E(N, r_s, r_c, v)}{N} \right]_{r_s = r_s^*} = 0 \qquad (9)$$

where the derivative is taken at constant N and $r_c = r_c(r_s^B, v)$, where r_s^B is the bulk density parameter. The core radius is fixed by the bulk stability condition, which is equation (9) in the limit $N \to \infty$. We have self-compression if $r_s^* < r_s^B$ and self-expansion if $r_s^* > r_s^B$.

The elastic stiffness of the cluster is defined by

$$B(N, r_s^*, r_c, \nu) = -V \frac{\partial^2 E}{\partial V^2}\bigg|_N = \frac{1}{12\pi r_s^* N} \frac{\partial^2}{\partial r_s^2} \left[\frac{E(N, r_s^*, r_c, \nu)}{N}\right]_{r_s = r_s^*}. \quad (10)$$

In the limit $N \to \infty$, this quantity goes over to the bulk modulus. Stability demands that $B \geqslant 0$.

On the other hand, the spherically averaged pseudopotential model (SAPS) takes into account the geometrical arrangement of the ions located at positions $\boldsymbol{R}_j$ [10, 11]. This is optimized by minimizing the total energy of the cluster.

Only valence electrons are treated explicitly, as in the SJM, with the ion cores being replaced by atomic pseudopotentials $w(|\boldsymbol{r} - \boldsymbol{R}_j|)$. The simplification introduced by the SAPS model for clusters of simple metals consists of replacing the external potential felt by the valence electrons, $V_+(\boldsymbol{r}) = \sum_j^{N_{at}} w(|\boldsymbol{r} - \boldsymbol{R}_j|)$, by its spherical average, $\langle V_+ \rangle (r)$, around the cluster centre. In this way, the energy functional in the SAPS model reads as

$$E_{SAPS}[n, \boldsymbol{R}_i] = T[n] + E_{xc}[n] + \frac{1}{2} \int d^3r \int d^3r' \frac{n(r)n(r')}{|\boldsymbol{r} - \boldsymbol{r}'|}$$
$$+ 4\pi r^2 \int dr \, \langle V_+ \rangle n(r) + \frac{1}{2} \sum_{i \neq j}^{N_{at}} \frac{z_i z_j}{|\boldsymbol{R}_i - \boldsymbol{R}_j|} \quad (11)$$

where z_i denotes the charge of the ions and $N_{at} = N/\nu$ is the number of atoms. The last term in equation (11) represents the repulsion between the ion cores, which is approximated by the interaction between point charges. As in the SJM, we have used the LDA with the correlation energy functional of Perdew–Wang.

In order to determine the cluster energy, we start from a random initial atomic configuration $\boldsymbol{R}_j^0$ and solve the Kohn–Sham equations, evaluating the valence electron density and the total energy given by equation (11). To obtain the geometry that minimizes the total energy, we calculate the energy variation $(\delta E_j)_\alpha$, corresponding to the displacement of the ion at position $\boldsymbol{R}_j$ in each Cartesian direction ($\alpha = x, y, z$), by a small quantity δd, keeping the electron density and the other ions' coordinates frozen. Then we choose the maximal energy variation δE_{max} and move each ion coordinate by an amount $[(\delta E_j)_\alpha/\delta E_{max}]\delta d$, obtaining a new geometry, $\boldsymbol{R}_j^1$, for which we calculate the corresponding electron density. With this new geometry we repeat the cycle again, and iterate the process until convergence is achieved and an equilibrium geometry is found. This generally leads to a local minimum. To find the global minimum we have repeated the calculations for a large number (typically 20) of random initial configurations.

To obtain the elastic stiffness in the SAPS model, we use an analogue of equation (10) with the approximation

$$\frac{\partial^2 E}{\partial r^2} \simeq \frac{E(\boldsymbol{R}_j - \delta\boldsymbol{r}) + E(\boldsymbol{R}_j + \delta\boldsymbol{r}) - 2E(\boldsymbol{R}_j)}{|\delta\boldsymbol{r}|^2}. \quad (12)$$

The energy of the cluster is calculated with the atoms at the equilibrium positions $\boldsymbol{R}_j$ and displaced radially in and out by a small amount, $\delta\boldsymbol{r}$, from $\boldsymbol{R}_j$ (for simplicity we have omitted the energy functional dependence on n).

An extension of the SAPS model which exploits all ionic degrees of freedom in three dimensions but restricts the electronic many-body problem to axial symmetry has been introduced recently by Montag and Reinhard [12, 13]. This model is known as CAPS (cylindrically averaged pseudopotential scheme), since a cylindrical average is taken instead of a spherical average.

In this work we compare the SAPS model with the SJM because the two schemes use a spherical average of the atomic pseudopotential and one could expect the two descriptions of some clusters properties to be similar. In particular, one could expect that the phenomena of self-compression of neutral clusters with respect to the bulk density and self-compression or self-expansion of charged clusters, which have been identified in the SJM [8, 9], to also be described in the SAPS. With this goal, we examine the two models for small clusters of sodium and aluminium. In the appendix we compare the LDA cohesive energies with the generalized gradient approximation (GGA) ones.

2. Results

Figure 1 shows the SAPS valence electron density for eight-atom clusters of sodium ($r_s = 3.93$, $v = 1$) and aluminium ($r_s = 2.07$, $v = 3$), in comparison with the SJM one, if the jellium edge is allowed to move. In the SAPS, we have used the recently proposed evanescent core pseudopotential model, which has the advantages of being local and analytical and which generally describes the main physical properties of bulk simple metals quite well [14–16]. In the SJM, we have used the simpler and more common Ashcroft pseudopotential with the core radius fixed by the condition of bulk stability. We could as well have used any other local pseudopotential with a single free parameter, arriving at the same results. We conclude that the two densities are somewhat different, especially in the interior for aluminium (the SAPS density is much lower there). The surface diffusivity is larger for SAPS than for SJM (this leads to a larger redshift of the surface plasmon resonance with respect to the Mie peak [17]). However, the radial probability density $r^2 n(r)$, represented in the inset, is similar in the two models. We have performed the same comparison for positively ionized systems (Na_8^{3+} and Al_8^{12+}), arriving at the same conclusions.

Let us consider the energy of the cluster in the two models. The cohesive energy is the difference between the energy of the free atom and the energy of the cluster per atom,

$$E_{coh}(N_{at}) = E(v) - \frac{E(v N_{at})}{N_{at}}. \tag{13}$$

For the bulk, equation (13) leads to the heat of sublimation: $E_{coh}(N_{at} = \infty) = E(v) - a_v v$, where a_v is the bulk energy per valence electron. Figure 2 represents the cohesive energy for small clusters of sodium and aluminium using the SAPS model and the two versions of the SJM: one with the self-compression effect and another with the background density frozen at the bulk value, r_s^B. In figure 2 we have also plotted the liquid drop energy in the SJM

$$E_{coh}^{LDM}(N_{at}) = a_s v^{2/3}(1 - N_{at}^{-1/3}) + a_c v^{1/3}(1 - N_{at}^{-2/3}) \tag{14}$$

with a_s and a_c the surface and curvature energy coefficients, respectively. In the case of self-compression, the curvature energy coefficient is replaced by [7]

$$\tilde{a}_c = a_c - \frac{1}{2} \frac{(a_s')^2}{a_v''}. \tag{15}$$

For sodium we have $\tilde{a}_c = 0.18$ eV and for aluminium $\tilde{a}_c = -0.10$ eV, which contrasts with the non-compression values of 0.26 and 0.65 eV, respectively. The surface energy ($a_s = 0.57$ eV for sodium and 0.86 eV for aluminium) is not affected by compression.

The cohesive energy in the SAPS is much lower than any of the SJM results, although a similar pattern (with maxima at shell closures) is apparent. For sodium, the self-compressed
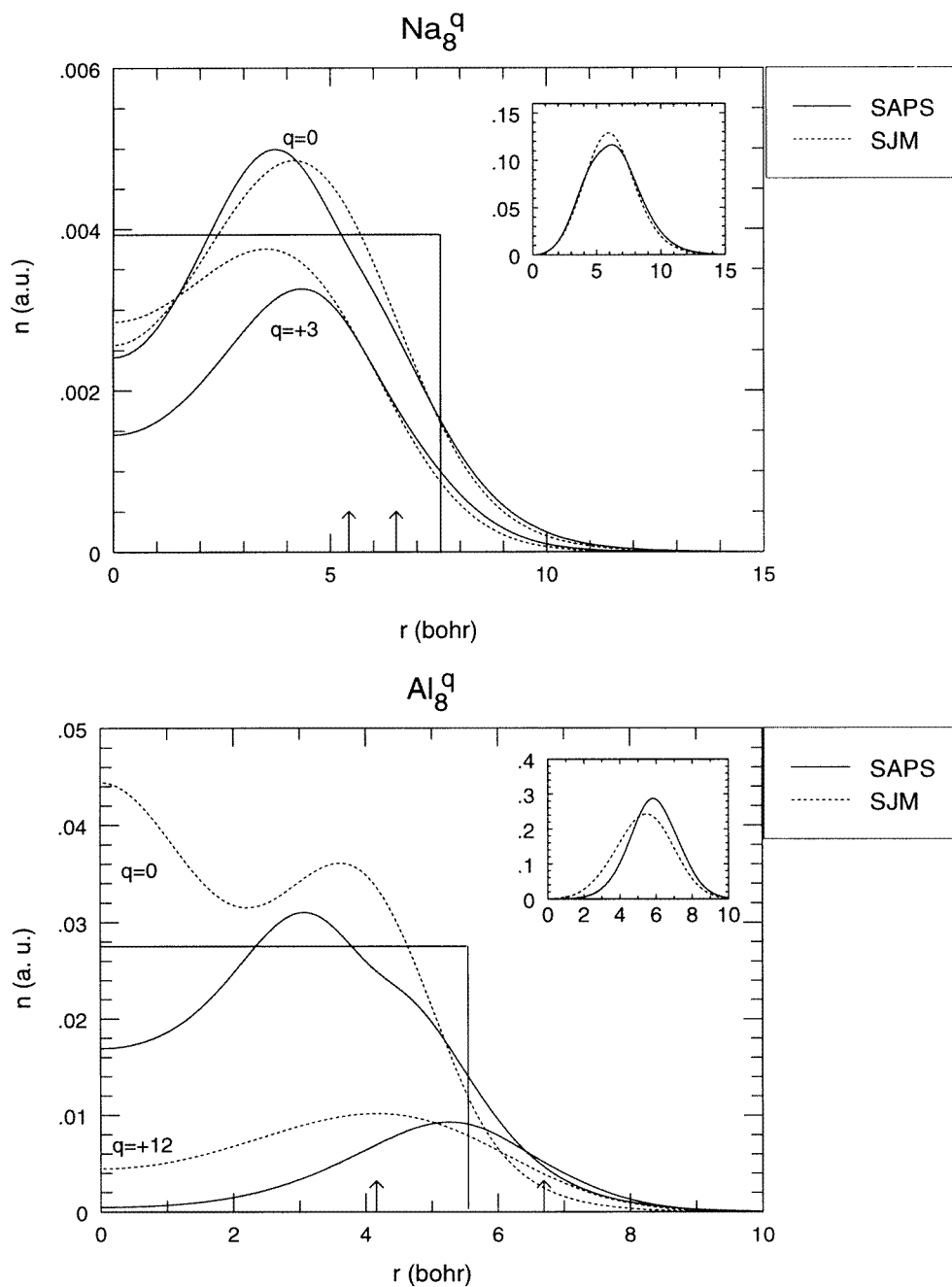
Figure 1. Valence electron densities of neutral and charged octamers of sodium and aluminium, obtained with the SAPS and the SJM. In the inset, we represent the radial probability density of the neutral clusters, $r^2 n(r)$, in arbitrary units. The horizontal line represents the background density of the neutral cluster in the SJM (its radius is $R_{\mathrm{jel}} = r_s^* N^{1/3}$, with $r_s^* = 3.70$ for sodium and $r_s^* = 1.92$ for aluminium. The vertical arrows on the horizontal axis denote the position of ionic shells in the SAPS: in each picture the left-hand arrow marks the position of the ionic shell for the neutral cluster, whereas the right-hand one stands for the charged case. Each cluster has a single ionic shell, with D_{4d} symmetry.
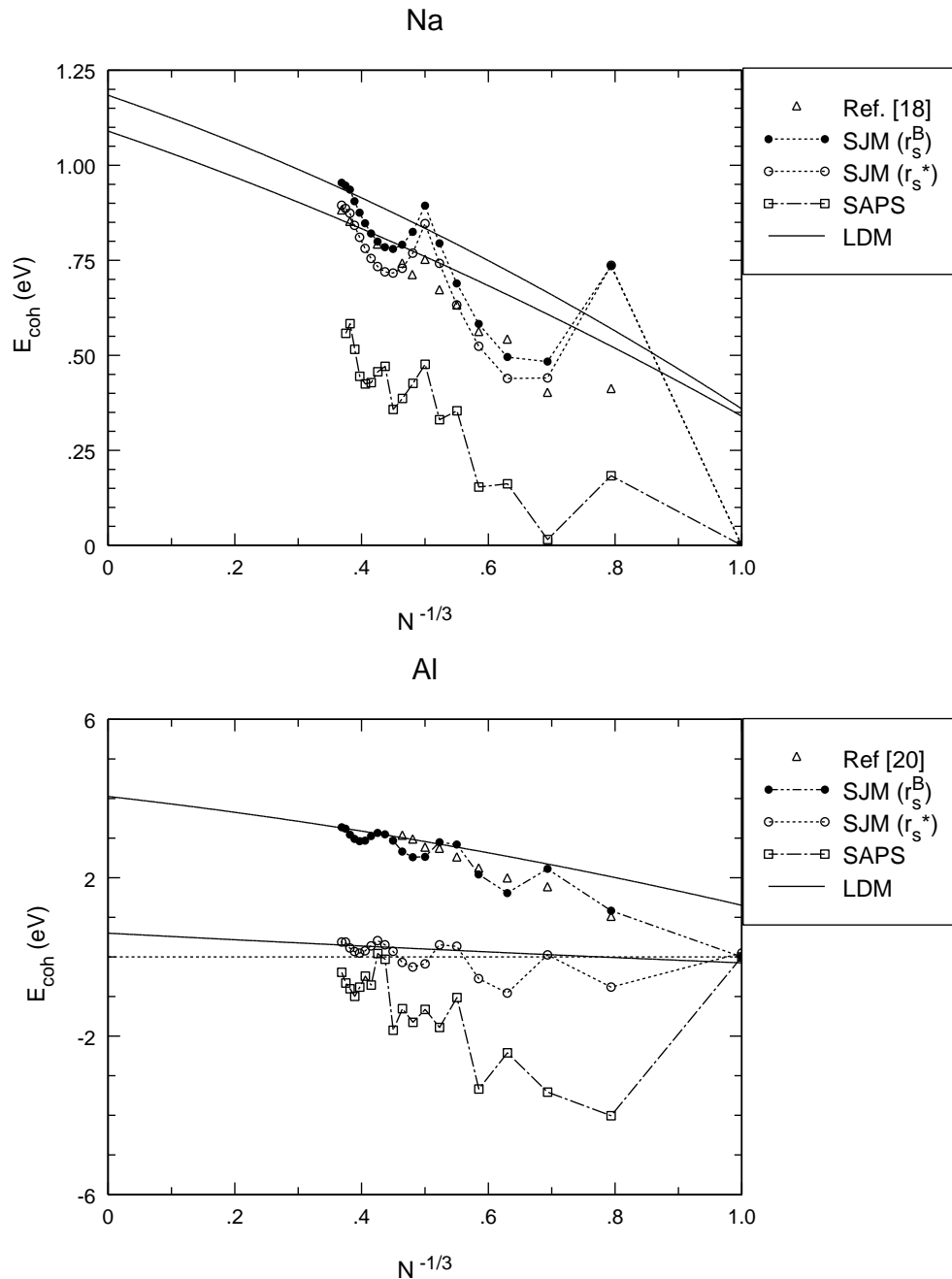
Na

Al

Figure 2. Cohesive energies of sodium and aluminium clusters obtained in the SAPS model and the SJM. The SJM is shown in two versions: one, denoted by SJM(r_s^B), with the background density fixed at the bulk value and another denoted by SJM(r_s^*) including self-compression, where the background density of the cluster is allowed to change. The full curves are obtained with the liquid drop formula, with (bottom) and without (top) the self-compression effect. (We take the Kohn–Sham energy of the atom instead of the liquid drop value.) Our results are compared with the Car–Parrinello calculations [18, 20].

SJM results are in very good agreement with LDA Car–Parrinello calculations [18] (and also close to the experimental values [19]). For aluminium, the frozen density SJM results are in good agreement with the Car–Parrinello calculations [20] (and experiment [21]), while self-compressed SJM and SAPS yield negative values for very small clusters. This fact should be seen as a drawback of the spherical approximation used in both models. The spherical restriction, valid for the atom, is indeed an artificial constraint for the bulk solid. This makes the SAPS valence-electron energies too high and the cohesive energies too low. In the SJM, the errors made for the atom and the solid seem to be similar.

The SAPS result for the cohesive energy depends somewhat on the selected pseudopotential, but replacing the evanescent core pseudopotential by a different one such as Manninen's [22] the SAPS results remain negative for small clusters. The error made in using the pseudopotential for the atom may be estimated by replacing the binding energy of the pseudo-atom by the sum of the first v ionization potentials in an all-electron calculation using the same exchange and correlation energies. That correction, using the evanescent core pseudopotential, yields an upwards shift in the cohesive energy of 0.2 eV for sodium and 0.0 eV for aluminium.
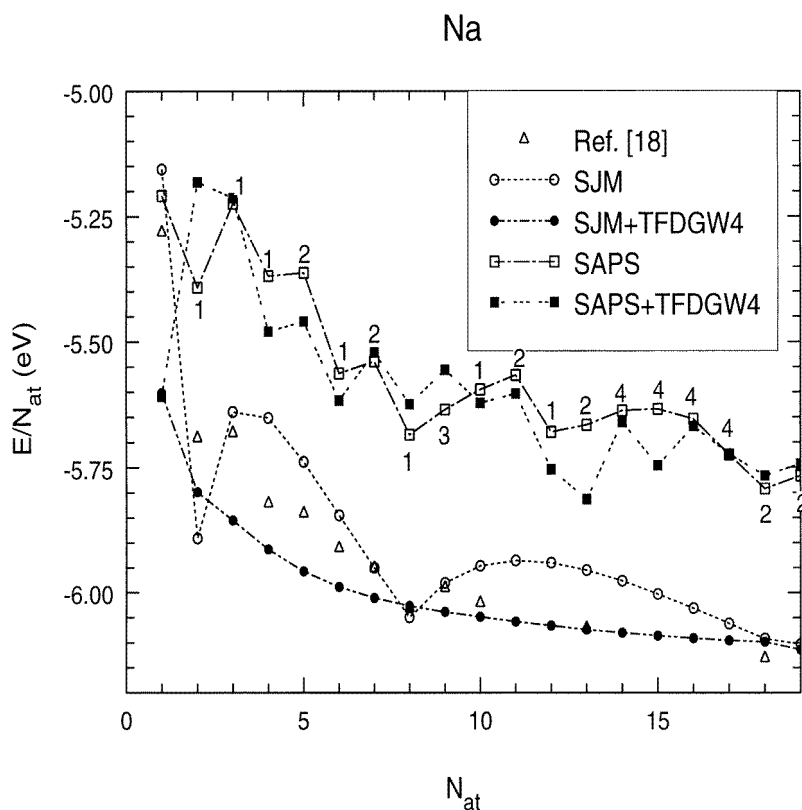

Figure 3. Binding energies per atom for sodium clusters in the SJM and SAPS models. The lines marked with TFDGW4 represents the energy obtained by replacing the quantal kinetic energy by the TFDGW4 functional of the Kohn–Sham density. The numbers denote the structure of ionic shells in SAPS and have the following meaning: 1, one ionic shell; 2, one ionic shell with one atom at the centre; 3, two ionic shells and 4, two ionic shells with one atom at the centre.

In the appendix, we compare the LDA with the GGA results for the cohesive energy, concluding that the density gradient corrections reduce this quantity.

Besides the electronic shell structure, leading to magic numbers, which appears in both the SJM and the SAPS model, in the latter there is an ionic structure which also reflects itself in oscillations of the total energy. In order to disentangle the electronic and geometric shell effects, we have evaluated the kinetic energy contribution by means of an extended Thomas–Fermi energy functional with fourth-order gradient corrections (TFDGW4) [23, 24] using, however, the self-consistent Kohn–Sham density of each model (figure 3). In this way the electronic shell structure due to the quantum kinetic energy operator of the Kohn–Sham equations is partially erased. In both cases it is clear that with the new functional we would obtain self-consistently a different ionic background and ionic structure, but we have just evaluated a semiclassical kinetic energy with the quantal density as in [24]. The resulting binding energies of sodium neutral clusters are represented in figure 3. In the SJM, we obtain a smooth curve, which may be fitted by a liquid drop formula; the surface and curvature coefficients are $a_s = 0.52$ eV and $a_c = 0.22$ eV, which agree very well with results obtained from the planar surface problem 0.58 eV and 0.26 eV, respectively [2]. But, in the SAPS, we are left with some wiggles, which are mainly due to the reorganization of ionic shells. An increase of the energy arises when a new shell is added. For instance, this happens when going from $N_{at} = 4$ to $N_{at} = 5$ or from $N_{at} = 13$ to $N_{at} = 14$. Note that, except for the $N_{at} = 1$ case, the SJM results are always above the SAPS results.

For the sake of comparing the cluster size evolution in the two models, we have plotted, in figure 4, the radius of the outer ionic shell R_{out} in SAPS divided by $R(N) = R_{jel}(N) - d/2$, where d is the distance between parallel close packed planes in the bulk solid, against the number of atoms. In fact, the planar surface is the limit of the curved surface of a large cluster and it is known from surface physics that the first lattice plane is located at a distance $x = -d/2$ from the jellium edge located at $x = 0$. The quantity $d = 1.436 r_0$ is the distance between the (110) planes in the bcc structure (these are the planes with the largest separation) and $d = 1.477 r_0$ is the distance between the (111) planes of the fcc structure. We see that R_{out}/R approaches 1 from above, although it becomes increasingly difficult to apply the SAPS to very large clusters and to attain the planar surface limit. This dilatation effect of the outer ion shell with respect to the surface limit is particularly clear for very small clusters. On the other hand, we observe contraction in the SJM: in figure 4, r_s^*/r_s^B goes from below to 1 when N_{at} increases. In both models, the approach to the asymptotic limit is more rapid for sodium than for aluminium.

Notwithstanding the expansion of the outer ionic shell, the distances between next-neighbour ions inside each shell are smaller than in the bulk environment differing from ionic shell to ionic shell. This inhomogeneous contraction observed in SAPS has been reported previously [25, 26]. Such an effect is outside the scope of the SJM, since the jellium background must have a constant density [1].

To analyse the behaviour of charged systems we may keep the size fixed (e.g. Na_8 and Al_8) and increase the charge all the way up to Coulomb explosion of the volume (figure 5). In the first case, the radius of the jellium sphere is increasing, while in the SAPS the same happens with the radii of the ionic shells. We see a strong similarity of the phenomenon of volume explosion described by the SJM and the SAPS model. The maximal positive charge that Na_8 can hold is $q = 3$, whereas for Al_8 it is $q = 13$ for the SJM and $q = 14$ for the SAPS (the charged systems of figure 1 are therefore close to their stability limit). For Al_8^+, we observe in both models a small self-compression instead of self-expansion with respect to the neutral system. This is an interesting effect since it goes against expectations.
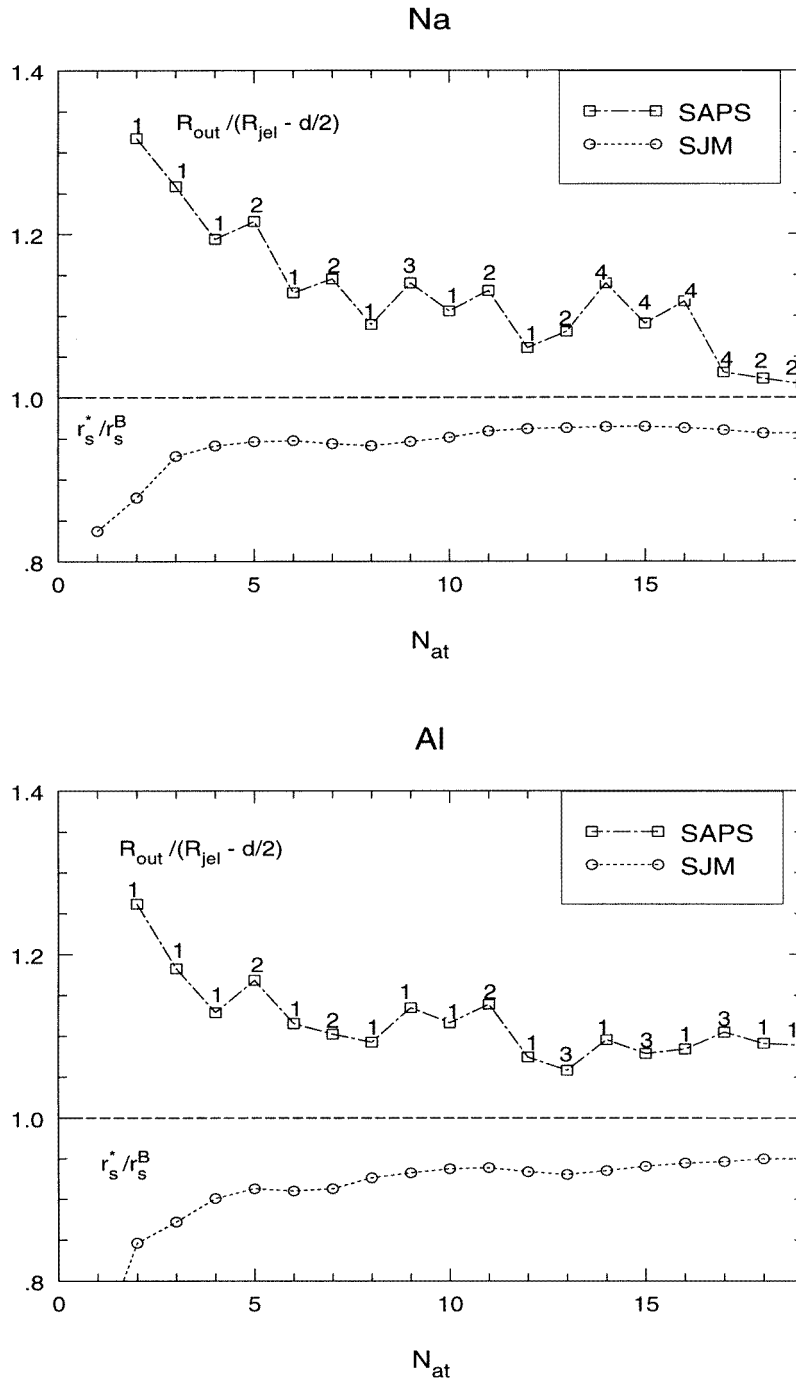
Figure 4. Size evolution of the outer ionic shell radius, $R_{\rm out}$, in the SAPS and of the equilibrium ionic density of SJM, r_s^*, for sodium clusters and aluminium. Both quantities are normalized to the corresponding limit $N \to \infty$. The numbers over the SAPS points have the same meaning as in figure 3.
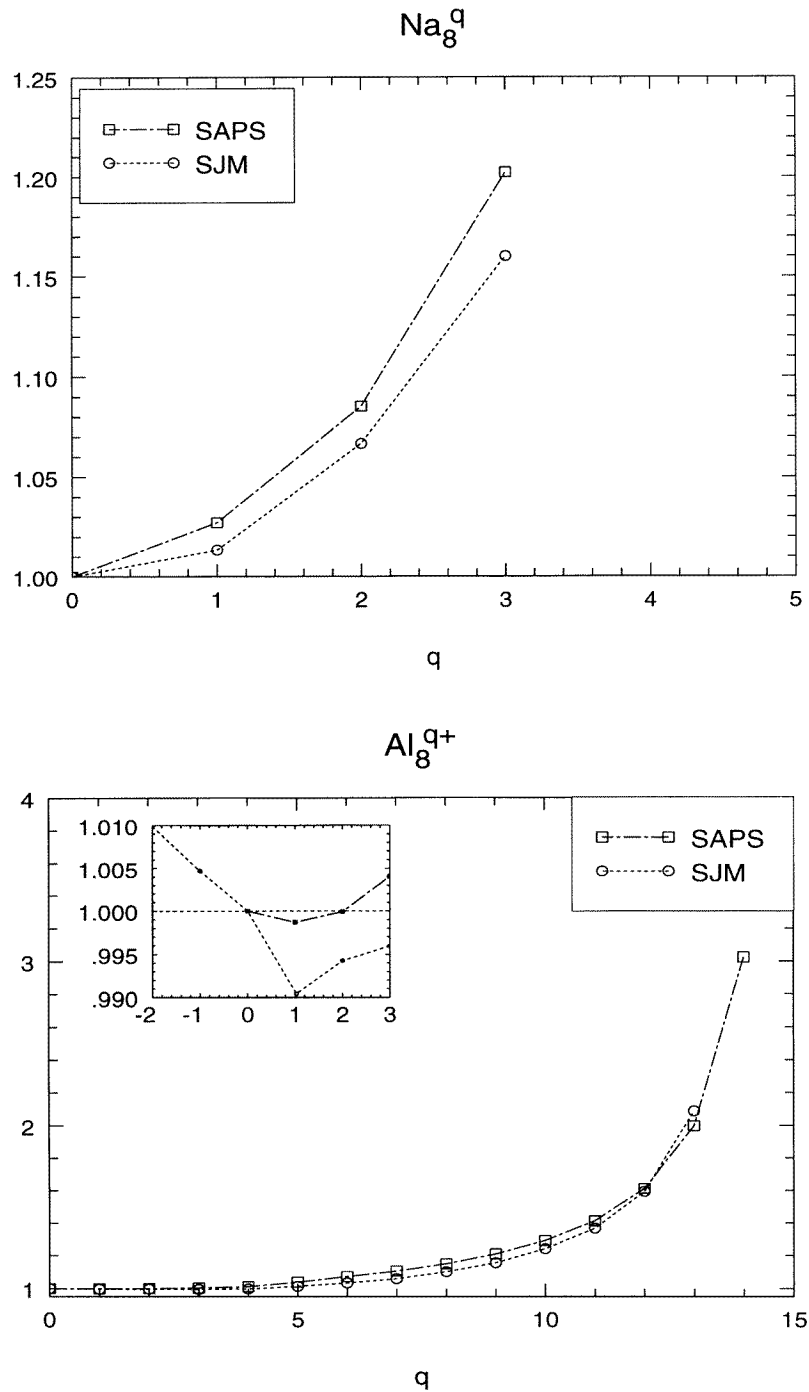
$$Na_8^q$$

$$Al_8^{q+}$$

Figure 5. Size of Na_8^{q+} and Al_8^{q+}, normalized to the corresponding size of the neutral system, as a function of charge q. For the SAPS we represent the ratio between the outer ionic shell radius of the charged and the neutral cluster. For the SJM we represent the ratio between the equilibrium density parameter, r_s^*, of the charged and the neutral cluster. The inset is a blow-up between $q = -2$ and $q = 3$ (for Al_8^{q+} the SAPS has no bound solutions for $q < 0$).
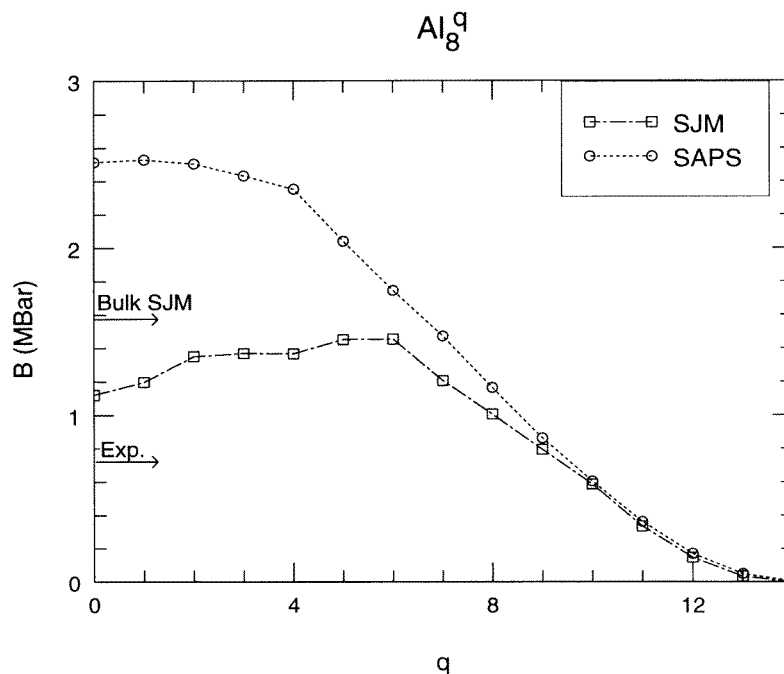
$$Al_8^q$$

Figure 6. Elastic stiffness B of Al_8^{q+}, as a function of charge q, obtained with the SAPS and the SJM models.

The type of instability we are describing is different from usual fission since, in the latter, the volume is fixed while the shape is deformed and here volume changes keeping the shape. The fissibility, defined as $x = E_C/2E_S$, where E_C is the Coulomb and E_S is the surface energy of a spherical cluster, controls the fission probability. For $x = 1$ the fission barrier vanishes and the cluster decays spontaneously. A different parameter should be considered for the explosion of the background. Anyway, within the SJM, we get $x = 3.4$ for Na_8 and $x = 26.6$ for Al_8 as critical fissibilities for volume explosion, which indicates that excited clusters prefer to lower their energy by deforming and breaking into two or more pieces than by exploding the volume.

Finally, in figure 6 we compare the elastic stiffness of charged aluminium clusters. The two values agree when the charge is large, but differ for small charges: the elastic stiffness of neutral aluminium clusters in the SAPS model is much larger than in the SJM model. We note that the aluminium bulk modulus given by the SJM is a factor of 2 larger than the experimental value, as indicated in the figure.

3. Conclusions

We have examined comparatively some physical properties of small clusters of sodium and aluminium as given by the SJM and the SAPS models.

The radial electronic probabilities are similar for sodium and somewhat different for aluminium. Although the SJM is conceptually and practically simpler, its results for

the cohesive energy are in better agreement with more involved theoretical results. The restriction to the spherical symmetry seems to be a serious drawback of the SAPS model. The outer ionic radius in the SAPS and the jellium edge in the SJM for neutral clusters approach the asymptotic limit in different ways. However, the results of the two models compare very well when we normalize the ionic radius of a charged cluster to that of the corresponding neutral cluster, and keep the number of atoms fixed when increasing the charge. The elastic stiffness given by the SJM, although too high in comparison with data for high density metals such as aluminium, is better than the SAPS output. This indicates that the spherical restriction to the ionic structure, besides giving too low a cohesive energy for high density metal clusters, also makes them too hard. Therefore, the corresponding monopole compression mode in the SAPS has an energy which is expected to be too high in comparison with experiment [27].

In conclusion, the results obtained with the SAPS for the energetics and compression properties of small clusters should be taken with some care. Simpler models, such as SJM, may surprisingly perform better. On the other hand, the SJM is useless for heterogeneous clusters, which SAPS is able to describe. The two types of models are useful for understanding the main trends of small and large clusters, since *ab initio* theoretical models are computationally more elaborate and, at present, almost impossible to apply to clusters with more than 20 atoms. Since the SJM and the SAPS models assume spherical symmetry, they are particularly suitable for systems with spherical geometries (for instance, $N_{at} = 8$ and 20 for sodium). They are not adequate for systems with $N_{at} \leqslant 5$, which are known, from first principles calculations, to be planar.

The assumptions of stabilized jellium are not restricted to a compact spherical shape, making it more versatile than the SAPS model for describing some properties of metallic clusters. A simple modification of the SJM which should bring it to a better agreement with SAPS is the hollow SJM [28, 29]. Indeed, for a small system, we may open a hole in the middle and vary the size of the system so that the energy is minimal for a given number of particles. Deformed jellium [30] and CAPS [12, 13] represent improvements of, respectively, spherical SJM and SAPS which correct the spherical approximation.

Appendix. The generalized gradient approximation for small clusters

The local density approximation (LDA) for exchange and correlation is the most used scheme in density functional theory, but other approximations, which try to correct some of its deficiencies (e.g. incapacity to bind extra electrons), may be implemented. One of the most popular is a semi-local approach called the generalized gradient approximation (GGA) from which there are a couple of versions, e.g. [31, 32]. Instead of LDA, we have used the GGA, in the form proposed recently by Perdew *et al* [32], for calculating the cohesive energies for sodium and aluminium clusters in the SJM as well as in the SAPS. In the SAPS we have taken the ionic configuration optimized within the LDA. For SJM we are not considering self-compression.

The results are shown in figure A1, in comparison with LDA theory and experimental data. We obtain a small decrease of the cohesive energy for both metals. This fact reiterates our conclusion, reached with the LDA, that the SJM is in better agreement with the experimental data than the SAPS. The decrease of the cohesive energy, due to gradient corrections, is a well known feature of density functional theory [31].
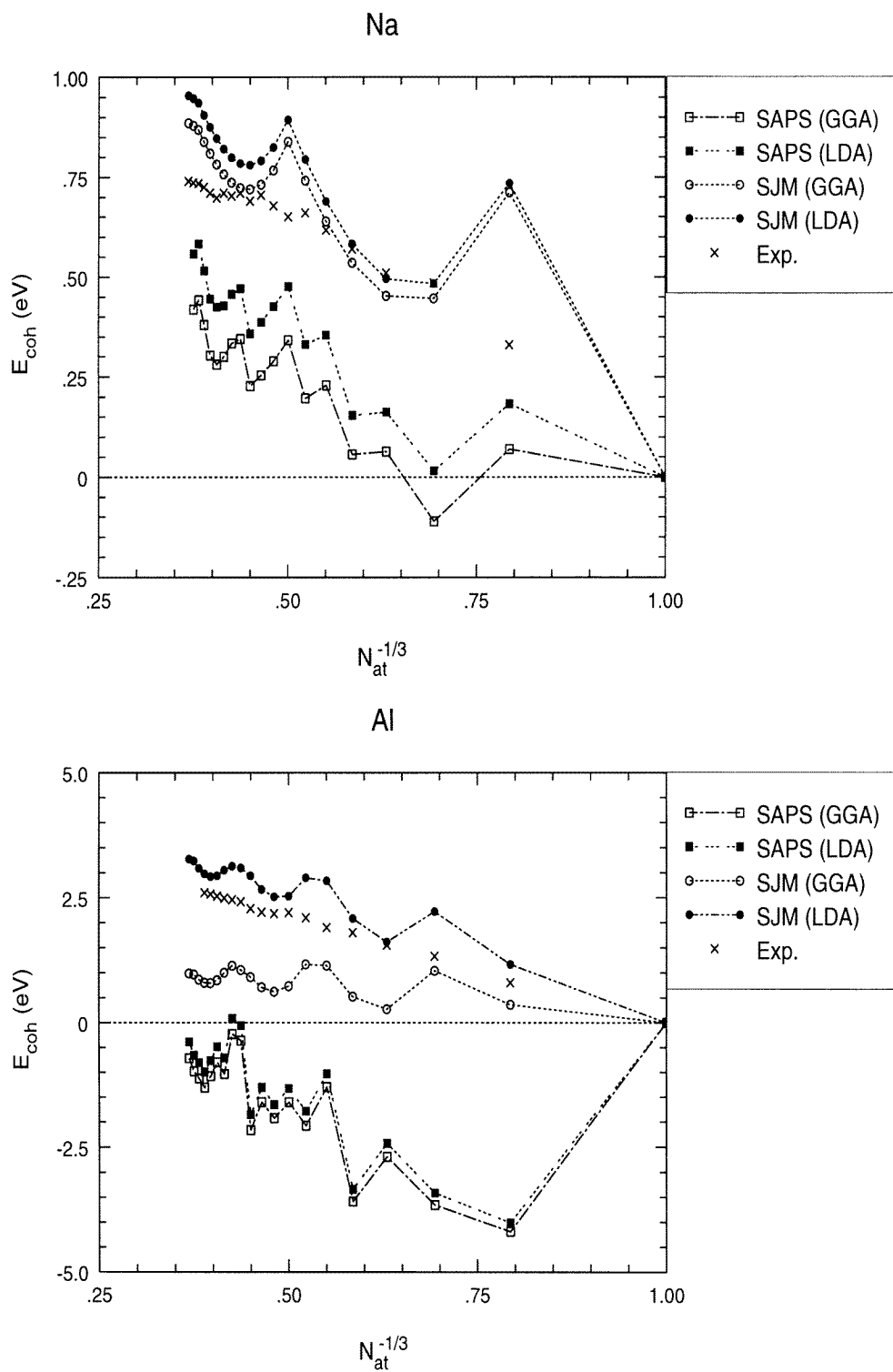
Figure A1. Cohesive energies of sodium (top) and aluminium (bottom) clusters obtained within the SAPS and the SJM, with the LDA and GGA for exchange and correlation.

Acknowledgments

References

[1] Perdew J P, Tran H Q and Smith E D 1990 *Phys. Rev.* B **42** 11 627
[2] Fiolhais C and Perdew J P 1992 *Phys. Rev.* B **45** 6207
[3] Brajczewska M, Fiolhais C and Perdew J P 1993 *Int. J. Quantum Chem.* **27** 249
[4] Perdew J P, Ziesche P and Fiolhais C 1993 *Phys. Rev.* B **47** 16 460
[5] Ashcroft N W 1966 *Phys. Lett.* **23** 48
[6] Perdew J P and Wang Y 1992 *Phys. Rev.* B **45** 13 244
[7] Perdew J P, Brajczewska M and Fiolhais C 1993 *Solid State Commun.* **88** 795
[8] Vieira A, Brajczewska M, Fiolhais C and Perdew J P 1996 *Int. J. Quantum Chem.* S **30** 325
[9] Brajczewska M, Vieira A, Fiolhais C and Perdew J P 1996 *Prog. Surface Sci.* **53** 1537
[10] Iñiguez M P, López M J, Alonso J A and Soler J 1989 *Z. Phys.* **11** 163
[11] Mañanes A, Iñiguez M P, López M J and Alonso J A 1990 *Phys. Rev.* B **42** 5000
[12] Montag B and Reinhard P G 1994 *Phys. Lett.* **193A** 380
[13] Montag B and Reinhard P G 1995 *Z. Phys.* D **33** 265
[14] Fiolhais C, Perdew J P, Armster S Q, MacLaren J M and Brajczewska M 1995 *Phys. Rev.* B **51** 14 001
[15] Nogueira F, Fiolhais C, He J, Perdew J P and Rubio A 1996 *J. Phys.: Condens. Matter* **8** 287
[16] Pollack L, He J, Perdew J P, Marques M, Nogueira F and Fiolhais C 1997 *Phys. Rev.* B **55** 15 544
[17] Brack M 1993 *Rev. Mod. Phys.* **65** 677
[18] Röthlisberger U and Andreoni W 1991 *J. Chem. Phys.* **94** 8129
[19] Bréchignac C, Cahuzac Ph, Leygnier J and Weiner J 1989 *J. Chem. Phys.* **90** 1492
[20] Jones R O 1991 *Phys. Rev. Lett.* **67** 224
[21] Ray U, Jarrold M F, Bower J E and Krauss J S 1989 *J. Chem. Phys.* **91** 2912
[22] Manninen M 1986 *Phys. Rev.* B **34** 6886
[23] Engel E and Perdew J P 1991 *Phys. Rev.* B **43** 1331
[24] Engel E, LaRocca P and Dreizler R M 1994 *Phys. Rev.* B **49** 16 728
[25] Mañanes A, Alonso J A, Lammers U and Borstel G 1991 *Phys. Rev.* B **44** 7273
[26] Glossman M D, Iñiguez M P and Alonso J A 1992 *Z. Phys.* D **22** 541
[27] Aguilar J G, Mañanes A, Duque F, López M J, Iñiguez M P and Alonso J A 1994 *Int. J. Quantum Chem.* **61** 613
[28] Membrado M, Pacheco A F and Sañudo J 1991 *Solid State Commun.* **77** 887
[29] Yannouleas C and Landman U 1994 *Chem. Phys. Lett.* **217** 175
[30] Hirschmann Th, Brack M and Meyer J 1994 *Ann. Phys., Lpz.* **3** 336
[31] Perdew J P, Chevary J A, Vosko S H, Jackson K A, Pederson M R, Singh D J and Fiolhais C 1992 *Phys. Rev.* B **46** 6671
[32] Perdew J P, Burke K and Ernzerhof M 1996 *Phys. Rev. Lett.* **77** 3865